Available online at www.sciencedirect.com
SCIENCE DIRECT®
Advances in Space Research 33 (2004) 1152–1159
ADVANCES IN SPACE RESEARCH (a COSPAR publication)
www.elsevier.com/locate/asr

Performance of the MODIS semi-analytical ocean color algorithm for chlorophyll-*a*

K.L. Carder [a,*], F.R. Chen [a], J.P. Cannizzaro [a], J.W. Campbell [b], B.G. Mitchell [c]

[a] Department of Marine Science, University of South Florida, 140 7th Avenue South, Saint Petersburg, FL 33701, USA
[b] Ocean Process Analysis Laboratory, University of New Hampshire, 39 College Road, Durham, NH 03824, USA
[c] Scripps Institution of Oceanography, 8602 La Jolla Shores Drive, La Jolla, CA 92037, USA

Received 27 February 2003; received in revised form 17 March 2003; accepted 7 April 2003

Abstract

The Moderate Resolution Imaging Spectroradiometer (MODIS) semi-analytical (SA) algorithm calculates the spectral absorption properties of surface waters, splitting them into those associated with phytoplankton, $a_{ph}(\lambda)$, colored dissolved organic matter or gelbstoff, $a_g(\lambda)$, and water, $a_w(\lambda)$. The phytoplankton absorption coefficient, $a_{ph}(675)$, is then used to derive the concentration of chlorophyll-*a*, Chlor_a_3. The SA algorithm is designed to respond to variable ratios of $a_{ph}(\lambda)$ to $a_g(\lambda)$ and to wide ranges in the chlorophyll-specific phytoplankton absorption coefficient, $a^*_{ph}(\lambda)$, for a given chlorophyll-*a* level. In this paper, the SA algorithm is expanded to include environments consistent with strong upwelling zones and high latitudes. Spatial and temporal differences in MODIS Terra chlorophyll-*a* retrievals are examined between Chlor_a_3 and an empirical algorithm, Chlor_a_2, developed to mimic the performance of the Sea-viewing Wide Field-of-View Sensor (SeaWiFS) OC-4 chlorophyll-*a* algorithm. The greatest differences observed are for upwelling regions and for southern high-latitude waters during austral spring where Chlor_a_2 values are on average about half of field and Chlor_a_3 values due to lower chlorophyll-specific phytoplankton absorption coefficients typical of this region. Preliminary match-up results indicate strong linearity and good agreement between in situ chlorophyll-*a* concentrations and MODIS-derived Chlor_a_3 compared to Chlor_a_2.

Keywords: Remote sensing; Chlorophyll; Imaging; Light absorption; Phytoplankton; Gelbstoff

1. Introduction

Chlorophyll-*a* concentration is the most widely used product derived from ocean-color data. The first such measurements were made with the Coastal Zone Color Scanner (CZCS) which operated between 1978 and 1986. The CZCS pigment concentrations were related to the sum of chlorophyll-*a* and phaeophytin-*a*, and an empirical spectral-ratio algorithm was used for the retrievals (Gordon and Morel, 1983). With improved spectral and radiometric resolution, the SeaWiFS sensor began producing global maps of chlorophyll-*a* concentration in September 1997, using an empirical, spectral-ratio algorithm (O'Reilly et al., 2000). Corrections for gelbstoff and detrital absorption that do not co-vary with chlorophyll-*a* were not made. Gelbstoff and detritus can absorb enough light at blue wavelengths to increase empirically retrieved chlorophyll-*a* concentrations by as much as a factor of two (Hu et al., 2000).

Empirical, spectral-ratio algorithms also do not correct for variations in the chlorophyll-specific phytoplankton absorption coefficient, $a^*_{ph}(\lambda)$. Tenfold variations in $a^*_{ph}(\lambda)$ can be found due to changes in phytoplankton assemblages and cell properties (Bricaud et al., 1995) between the nutrient-poor, photon-rich subtropical gyres and nutrient-rich, photon-poor upwelled or high-latitude waters. As a result, CZCS (Mitchell and Holm-Hansen, 1991) and SeaWiFS (Moore et al., 1999) pigment retrievals south of 50°S have been underestimated by as much as a factor of two. Since most primary production algorithms are directly dependent upon chlorophyll-*a* (Behrenfeld and Falkowski,

* Corresponding author. Tel.: +1-727-553-3952; fax: +1-727-553-3918.
E-mail address: kcarder@monty.marine.usf.edu (K.L. Carder).

0273-1177/$30 © 2003 COSPAR. Published by Elsevier Ltd. All rights reserved.
doi:10.1016/S0273-1177(03)00365-X

1997; Howard and Yoder, 1997), this suggests that until now some satellite-derived primary-production estimates for the Southern Ocean may be as little as 50–60% of the actual values during austral spring (Esaias et al., 2003). If true, this would also directly impact the flux of carbon to the deep ocean south of 50°S.

A different approach is to use a semi-analytical (SA) model to separate the pigment absorption components from those due to degradation products (e.g. gelbstoff and detritus) and to adjust the chlorophyll-specific phytoplankton absorption coefficient on the basis of chlorophyll-*a* concentration and nutrient and light sufficiency (Carder et al., 1999). Separation of the effects of the major components is achieved using the spectral differences between $a_{\mathrm{ph}}(\lambda)$ and $a_{\mathrm{g}}(\lambda)$. In reality, $a_{\mathrm{g}}(\lambda)$ also includes absorption due to particulate detritus, which has a similar spectral shape (Roesler et al., 1989). By comparing the sea-surface temperature to the nitrate-depletion temperature (NDT) (Kamykowski, 1987), the presence of large, chlorophyll-rich cells and small, chlorophyll-poor cells can be deduced from space (Carder et al., 1999). Chlorophyll-rich cells with low $a^*_{\mathrm{ph}}(\lambda)$ values (packaged pigments) are generally present in photon-poor, nutrient-replete environments whereas chlorophyll-poor cells with high $a^*_{\mathrm{ph}}(\lambda)$ values (unpackaged pigments) are present in photon-rich, nutrient-deplete environments. The NDT for any region of the ocean is the temperature above which nitrate is negligible.

2. Background

MODIS is a 36-band spectrometer observing the land, atmosphere, and oceans of the Earth between 412 to 14,385 nm (Esaias et al., 1998). The first images from MODIS Terra were acquired 24 February 2000, and a major reprocessing of ocean data (Collection 4) was completed in September 2002. This collection contained data that had been vicariously recalibrated and processed with the most recent versions of various algorithms. The most stable time period for MODIS occurred after November 2000, and vicarious calibrations have been applied to data through until February 2002. Therefore, only data from this time period are considered by this contribution.

Chlorophyll-*a* concentrations that are derived semi-analytically (Chlor_a_3) differ from other approaches for retrieving chlorophyll-*a* concentrations as the spectrum of $a^*_{\mathrm{ph}}(\lambda)$ is adjusted dynamically using MODIS-derived sea-surface temperatures, SST (Carder et al., 1999). Comparing SST to the nitrate-depletion temperature (Kamykowski, 1987) as an indicator of nutrient availability provides a space-based cue for evaluating whether upwelling or convective overturn has replenished the surface waters with nutrients from below the surface mixed layer. This changes the species and pigment composition of the phytoplankton assemblage observed, thus requiring adjustments in $a^*_{\mathrm{ph}}(\lambda)$. These adjustments also compensate for the pigment package effect whereby increased cell size and pigment per cell decreases $a^*_{\mathrm{ph}}(\lambda)$ (Morel and Bricaud, 1981) (Fig. 1).

Note, however, that this NDT scheme also works when light (Mitchell et al., 1991) or iron (Sedwick et al., 2002) limit phytoplankton growth as in some high-latitude, nitrate-replete waters. These factors require similar adjustments in $a^*_{\mathrm{ph}}(\lambda)$ compared to when nitrate is the limiting factor (Moisan and Mitchell, 1999). In addition, an increase in average cell size from subtropical to polar waters (Odate and Maita, 1988) can contribute to increased pigment packaging in high-latitude waters, thus requiring lower $a^*_{\mathrm{ph}}(\lambda)$. This is caused by a decreased abundance of cyanobacteria, a major component of the picoplankton community, when water temperatures are less than 10 °C (Murphy and Haugen, 1985). Since global biogeographic boundaries coincide with nitrate-depletion temperature boundaries, our NDT scheme for adjusting $a^*_{\mathrm{ph}}(\lambda)$ seems to work even though factors other than nitrate can influence pigment packaging.

Adjustments for both gelbstoff and detrital absorption and for regional and temporal changes in the chlorophyll-specific phytoplankton absorption coefficients can remove the large biases produced by historical empirical algorithms for chlorophyll-*a* and subsequent primary-production fields. In this paper, the semi-analytical algorithm of Carder et al. (1999) is expanded to include environments consistent with strong upwelling zones and high latitudes. Chlorophyll-*a* data from MODIS Terra (Collection 4), derived by the semi-analytical algorithm, Chlor_a_3, and the empirical, Sea-WiFS-simulator algorithm, Chlor_a_2, are then compared to match-up field data for the period from January to June 2001. These comparisons are used to provide initial validation statistics for the two products representative of the time period November 2000 to February 2002 when sensor performance was stable and radiance data were well calibrated.

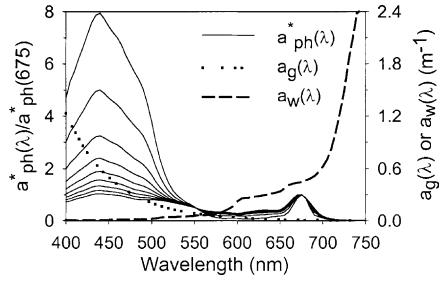

Fig. 1. Representative chlorophyll-specific phytoplankton absorption spectra, $a_{\mathrm{ph}}(\lambda)$, normalized at 675 nm. $a_{\mathrm{ph}}(\lambda)/a_{\mathrm{ph}}(675)$ decreases with increasing $a_{\mathrm{ph}}(\lambda)$ and increasing pigment packaging. Water (dashed; Pope and Fry, 1997) and typical gelbstoff (dotted) absorption spectra are shown for comparison.

3. Theoretical considerations

Remote-sensing reflectance, $R_{rs}(\lambda)$, is the ratio of water-leaving radiance, $L_W(\lambda)$, to downwelling irradiance, $E_d(\lambda)$, just above the sea surface. It is directly proportional to the backscattering, b_b, and inversely proportional to the sum of the absorption, a, and the backscattering coefficients (Morel and Prieur, 1977; Carder et al., 1999),

$$R_{rs}(\lambda) = \frac{L_w(\lambda)}{E_d(\lambda)} = \frac{f(\lambda)t^2}{Q(\lambda)n^2}\frac{b_b(\lambda)}{[a(\lambda)+b_b(\lambda)]}. \quad (1)$$

As the radiance-distribution factor f/Q is only weakly spectral for most satellite observation geometries (Morel and Gentili, 1993) and because the air-sea transmittance, t, and the index of refraction of seawater, n, are constants, Eq. (1) can be shortened to

$$R_{rs}(\lambda) \cong \text{const}\frac{b_b(\lambda)}{a(\lambda)+b_b(\lambda)}. \quad (2)$$

Also, since $b_b \ll a$ for most ocean waters (Morel and Prieur, 1977), spectral ratios of Eq. (2) can be directly interpreted in terms of the spectral ratios of backscattering and absorption.

The backscattering coefficient can be spectrally partitioned into components due to water and particles (i.e. phytoplankton and detritus) and the absorption coefficient can be spectrally partitioned into components due to water, phytoplankton, detritus, and gelbstoff:

$$b_b(\lambda) = b_{bw}(\lambda) + b_{bp}(\lambda), \quad (3)$$

$$a(\lambda) = a_w(\lambda) + a_{ph}(\lambda) + a_d(\lambda) + a_g(\lambda). \quad (4)$$

The spectral values of backscattering (Morel, 1974) and absorption (Pope and Fry, 1997) by pure water were used.

Particulate backscattering, b_{bp}, can be modeled using a hyperbolic function following the Angstrom law (Carder et al., 1999):

$$b_{bp}(\lambda) = X\left[\frac{551}{\lambda}\right]^Y, \quad (5)$$

where

$$X = X_0 + X_1 R_{rs}(551) \quad \text{and} \quad Y = Y_0 + Y_1\frac{R_{rs}(443)}{R_{rs}(488)} \quad (6)$$

and X_0, X_1, Y_0, and Y_1 are empirical constants derived using linear regression.

Absorption by detrital and gelbstoff components are combined as gelbstoff since they have similar exponential spectral shapes (Roesler et al., 1989) and can be modeled as follows:

$$a_g(\lambda) = a_g(400)\cdot e^{-S(\lambda-400)}, \quad (7)$$

where S is the spectral slope.

Phytoplankton absorption spectra can be written as a function of $a_{ph}(675)$ (Carder et al., 1999)

$$a_{ph}(\lambda) = a_{ph}(675)\cdot a_0(\lambda) \times \exp\left[a_1(\lambda)\tanh\left[a_2(\lambda)\ln\left(\frac{a_{ph}(675)}{a_3(\lambda)}\right)\right]\right], \quad (8)$$

where $a_0(\lambda)$, $a_1(\lambda)$, $a_2(\lambda)$, and $a_3(\lambda)$ are empirical constants derived by minimizing the errors between modeled and measured $a_{ph}(\lambda)/a_{ph}(675)$. Regions with high light and low nutrients in which phytoplankton are found with unpackaged pigments exhibit a relatively high hyperbolic tangent relationship as derived in Carder et al. (1999) compared to photon-poor, nutrient-replete polar and upwelling areas (Fig. 2).

Combining Eqs. (2)–(8) and using spectral $R_{rs}(\lambda)$ ratios of 412:443 and 443:551 which eliminates the constant term in Eq. (2), the two unknowns, $a_g(400)$ and $a_{ph}(675)$, can be solved for algebraically given values for the parameters X_0, X_1, Y_0, Y_1, S, and $a_{0\text{–}3}(\lambda)$ (Carder et al., 1999). The semi-analytical chlorophyll-a concentration is then derived from $a_{ph}(675)$ as follows:

$$[chl\ a]_{sa} = P_0\cdot[a_{ph}(675)]^{P_1}, \quad (9)$$

where P_0 and P_1 are empirically derived constants.

When $a_{ph}(675)$ is greater than 0.03 m^{-1}, though, which is equivalent to $[chla]_{sa} \sim 1.5$–2.0 mg m^{-3}, $R_{rs}(412)$ and $R_{rs}(443)$ are too low for accurate semi-analytical retrievals, and so the algorithm defaults to an empirical expression

$$[chl\ a]_{emp} = 10^{c_0+c_1\log(r_{35})+c_2[\log(r_{35})]^2+c_3[\log(r_{35})]^3}, \quad (10)$$

where $r_{35} = R_{rs}(488)/R_{rs}(551)$ and c_0, c_1, c_2, and c_3 are empirically derived constants. In order to provide a smooth transition between semi-analytical (sa) and empirical (emp) values, a weighting expression is applied

$$[chl\ a] = w_c[chl\ a]_{sa} + (1-w_c)[chl\ a]_{emp} \quad (11)$$

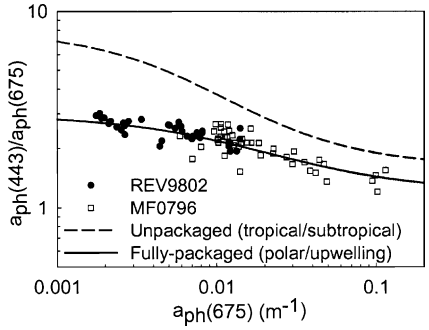

Fig. 2. Regional variation in $a_{ph}(443)/a_{ph}(675)$ versus $a_{ph}(675)$. Fully packaged data from the Antarctic Polar Frontal Zone (REV9802) and the Bering Sea (MF0796) regions are compared with high-light tropical and subtropical unpackaged data (Carder et al., 1999).

Table 1
Wavelength-dependent parameters for the semi-analytical chlorophyll-*a* algorithm for regions with unpackaged (UP) and fully packaged (FP) pigments

	Wavelength									
	412		443		488		510		551	
	UP	FP	UP	FP	UP	FP	UP	FP	UP	FP
a_0	2.2	1.02	3.59	1.89	2.27	1.24	1.40	0.84	0.42	0.32
a_1	0.75	0.26	0.80	0.45	0.59	0.42	0.35	0.36	−0.22	−0.08
a_2	−0.50	−0.45	−0.50	−0.45	−0.50	−0.45	−0.50	−0.45	−0.50	−0.45
a_3	0.0112	0.0210	0.0112	0.0210	0.0112	0.0210	0.0112	0.0210	0.0112	0.0210

when $a_{ph}(675)$ values are 0.015–0.030 m^{-1}. The chlorophyll weighting factor is $w_c = [0.03 - a_{ph}(675)]/0.015$ (Carder et al., 1999).

Parameters for the previously defined unpackaged pigment regime (Carder et al., 1999) and the recently derived fully packaged pigment regime are listed in Tables 1 and 2. For regions containing phytoplankton with packaging properties that fall between these two pigment regimes, the algorithm is run using parameters for each of the two packaging end members, and the results are blended as follows:

$$[chl\ a] = w_p[chl\ a]_{UP} + (1 - w_p)[chl\ a]_{FP}, \quad (12)$$

where $[chl\ a]_{UP}$ is the unpackaged value, $[\text{chl } a]_{FP}$ is the fully packaged value, and $w_p = [1.0 + (SST - NDT)]/5.0$ is the package weighting factor used for blending. The weighting function, w_p, is illustrated by Fig. 3, where the difference between SST and NDT is used to estimate nutrient availability and light history. The empirical relationship in Fig. 3 provided the lowest errors when comparing modeled versus measured chlorophyll-*a* concentrations for data adjacent to a strong upwelling event in April 1997 in the California Current (Fig. 4(c)). For regions outside the transitional domain, the fully packaged parameterization is used for low SSTs, and the unpackaged parameterization is used for high SSTs, relative to the nitrate depletion temperature.

Table 2
Wavelength-independent parameters for the semi-analytical chlorophyll-*a* algorithm for regions with unpackaged (UP) and fully packaged (FP) pigments

Parameter	UP	FP
X_0	−0.00182	−0.00182
X_1	2.058	2.058
Y_0	−1.13	−1.13
Y_1	2.57	2.57
S	0.0225	0.0170[a]
P_0	51.9	79.4
P_1	1.00	1.00
c_0	0.28	0.51
c_1	−2.78	−2.34
c_2	1.86	0.40
c_3	−2.39	0.00

[a] A gelbstoff slope, S, of 0.0170 is used for Antarctic fully packaged data only. The slope for Arctic fully packaged data remains 0.0225.

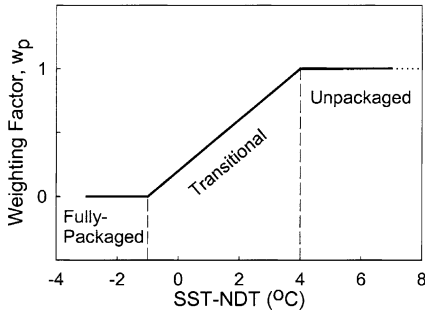

Fig. 3. Blending scheme to transition from fully packaged to unpackaged pigment parameterization.

4. Results and discussion

4.1. Shipboard data

The need for adjusting the package effect is best manifested in data from upwelling and high-latitude regions. California Current and Southern Ocean ship radiometry data (Table 3) were used to derive chlorophyll-*a* concentrations using both the empirical (Chlor_a_2) and semi-analytical (Chlor_a_3) algorithms that are then compared to in situ values (Fig. 4). The log–log linear regression results were linearized by the equation

$$[chl\ a]_{mod} = A \cdot ([chl\ a]_{in\ situ})^B. \quad (13)$$

Note that both Chlor_a_2 data trends (Figs. 4(a) and (b)) are biased below the 1:1 line, registering only 55% for values near 1 mg m^{-3} for the Southern Ocean. This is no surprise as Moore et al. (1999) and Mitchell and Holm-Hansen (1991) have found that SeaWiFS and CZCS empirical algorithms developed with largely northern mid-latitude data underestimate Southern Ocean data by about a factor of two. Similar trends have been observed for northern high latitudes (Maynard and Clark, 1987) and upwelling sites (Smyth et al., 2002).

In contrast, the performance of the SA algorithm with adjustment for pigment packaging is excellent for both the California Current upwelling data and for the Southern Ocean data (Figs. 4(c) and (d)). This supports

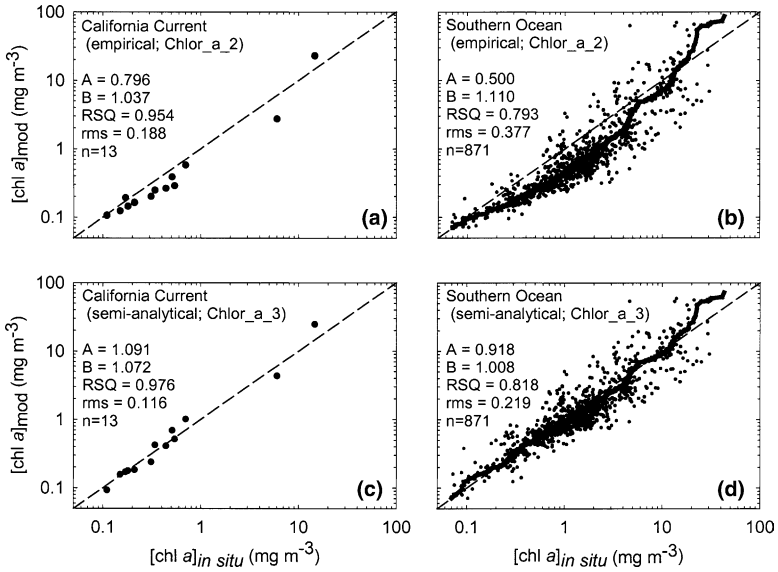

Fig. 4. Relationship between in situ [chl *a*] and empirically (Chlor_a_2) and semi-analytically (Chlor_a_3) derived [chl *a*] from shipboard radiometry data for (a and c) the California Current (April 1997) and (b and d) Southern Ocean (1991–2001). Dashed lines are one-to-one lines. Solid lines are quantile–quantile lines.

Table 3
USF and SeaBASS data sources, dates and locations

Cruise	P. Investigator	Institution	Dates	Location	*n*
CALCOFI	Carder, K.	USF	4/97	California Current	13
ROAVERRS97	Arrigo, K.	NASA/GSFC	12/97-1/98	Ross Sea	32
NBP9711	Mitchell, B.G.	UCSD/SIO	11/97-12/97	Ross Sea	20
REV9801	Mitchell, B.G.	UCSD/SIO	1/98	Antarctic Polar Frontal Zone	9
REV9802	Mitchell, B.G.	UCSD/SIO	2/98	Antarctic Polar Frontal Zone	2
AMLR2000	Mitchell, B.G.	UCSD/SIO	2/00-3/00	N. of Antarctic Peninsula	21
AMLR2001	Mitchell, B.G.	UCSD/SIO	2/01-3/01	N. of Antarctic Peninsula	29
LTER	Smith, R.	UCSB	1991-1999	W. of Antarctic Peninsula	758

the findings of Smyth et al. (2002) who used the Carder et al. (1999) semi-analytical algorithm with both ship and SeaWiFS data for the upwelling zone in the Iberian Sea. They found a nearly 1:1 relationship for SA chlorophyll-*a* measurements with little bias. They also found that an empirical algorithm developed for other upwelling areas (Kahru and Mitchell, 1999) performed well off the Iberian peninsula, but transitioning this algorithm to other regions was not addressed.

4.2. Satellite data

While low-latitude equatorial waters exhibit similar average mean chlorophyll-*a* concentrations for Chlor_a_2 (0.29 mg m^{-3}) and Chlor_a_3 (0.27 mg m^{-3}) (Table 4), Chlor_a_3 retrievals are higher in the eastern equatorial Pacific (Fig. 5) due to upwelling as expected based on Fig. 4. Average mean chlorophyll-*a* values for mid-latitude waters in the southern hemisphere are

Table 4
MODIS Terra monthly mean chlorophyll-*a* concentrations (mg m^{-3})

Date	60°S–35°S		35°S–15°S		15°S–15 °N		15°N–35°N		35°N–60°N	
	Chlor_a_2	Chlor_a_3	Chlor_a_2	Chlor_a_3	Chlor_a_2	Chlor_a_3	Chlor_a_2	Chlor_a_3	Chlor_a_2	Chlor_a_3
Dec.-00	0.35	0.72	0.17	0.17	0.30	0.31	0.36	0.29	0.67	0.78
Mar.-01	0.31	0.36	0.18	0.14	0.29	0.26	0.39	0.37	0.71	0.97
Jun.-01	0.27	0.31	0.19	0.15	0.29	0.24	0.27	0.21	1.31	1.27
Sept.-01	0.27	0.41	0.20	0.22	0.29	0.28	0.37	0.26	1.08	0.88
Average	0.30	0.45	0.18	0.17	0.29	0.27	0.35	0.28	0.94	0.97

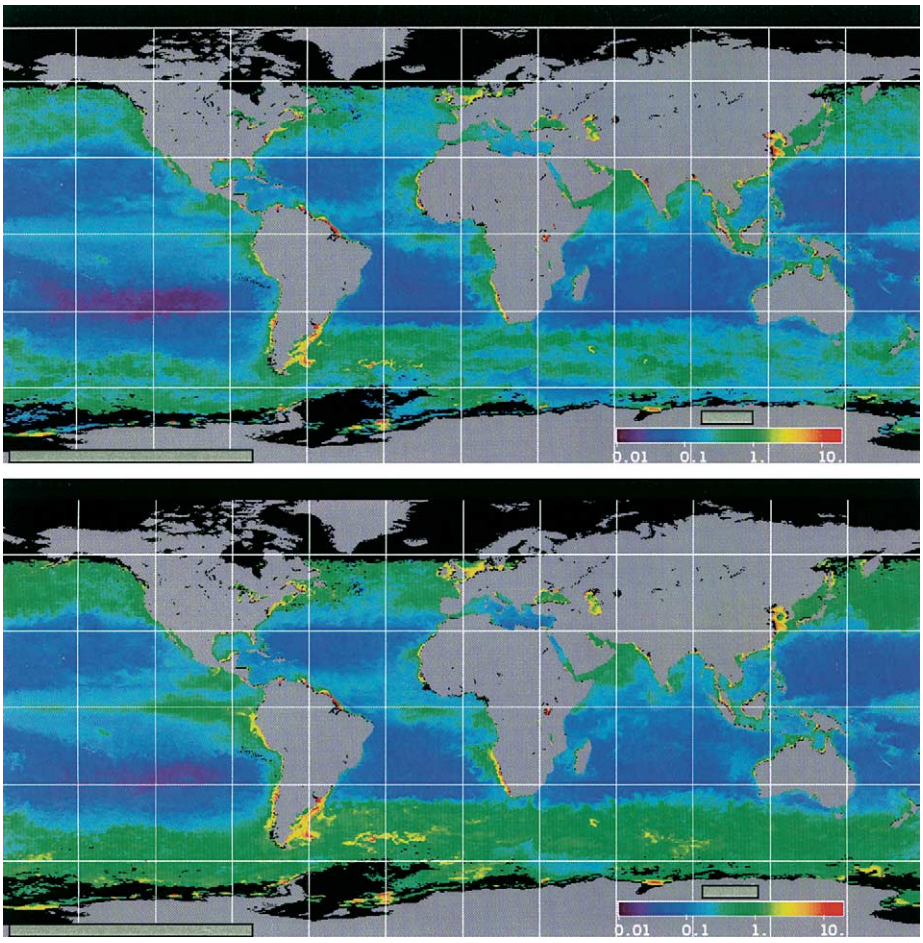

Fig. 5. Global maps (December 2000) of chlorophyll-*a* concentration (mg m^{-3}) composited in 39 km bins retrieved using empirical (Chlor_a_2, top) and semi-analytical (Chlor_a_3, bottom) algorithms from MODIS Terra radiometry.

similar for Chlor_a_2 (0.18 mg m^{-3}) and Chlor_a_3 (0.17 mg m^{-3}), but Chlor_a_2 values are higher in the northern hemisphere. Gelbstoff-rich runoff from northern rivers enriches water color, possibly increasing perceived chlorophyll-*a* retrieved by Chlor_a_2. Chlor_a_3 spectrally partitions this type of component from chlorophyll-*a*, effectively minimizing the influence of river runoff on pigment overestimates. Monthly mean values for southern high-latitude waters are similar for March and June, but Chlor_a_2 is only 50% of Chlor_a_3 during austral spring (Fig. 5, Table 4), largely due to the package effect (Fig. 2). Northern high-latitude monthly mean chlorophyll-*a* retrievals also exhibit larger Chlor_a_3 values in the spring due to pigment packaging. Differences between Chlor_a_2 and Chlor_a_3 values in this region, however, are smaller than for southern high latitudes as gelbsloff-rich runoff offsets the effects of pigment packaging (Sathyendranath et al., 2001).

The validity of Chlor_a_2 and Chlor_a_3 data was evaluated using match-ups with ship data from the SeaWiFS SeaBASS data archive (Werdell and Bailey, 2002). Chlorophyll-*a* data (1 km) from MODIS Terra were compared to ship data following the general match-up exclusion protocol of McClain et al. (2000), but only high quality (level zero) MODIS chlorophyll-*a* data were used. This eliminated data from shoal areas (<30 m) and provided cloud-free data collected within three hours of the satellite overpass. Furthermore, for selected pixels within 100 pixels of the scene edge, 5-by-5 pixel means rather than traditional 3-by-3 median values were used to improve signal-to-noise ratios. Field chlorophyll-*a* values within the top 10 m were averaged for comparison with satellite retrievals.

Global match-up results are presented in Fig. 6 for the Antarctic, Equatorial Pacific, California Current, western mid-Pacific, and the West Florida Shelf from January to June 2001. Note that both Chlor_a_2 (RMS = 0.174) and Chlor_a_3 (RMS = 0.170) are more accurate than the OC4v4 algorithm (RMS = 0.222) update (O'Reilly et al., 2000) which used an expanded global field of data. Ideally, for a 1:1 line, $A = B = 1.0$. Although the RMS error values for the two algorithms are similar, Chlor_a_3 values for A and B are much closer to 1.0. This suggests that the error due to

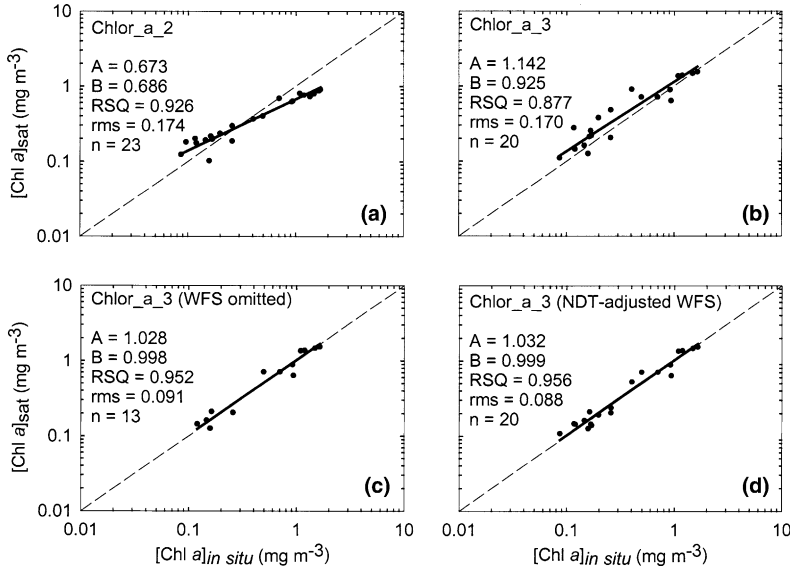

Fig. 6. Relationships between in situ [chl *a*] and MODIS-derived [chl *a*] using (a) Chlor_a_2, (b) Chlor_a_3, (c) Chlor_a_3 without the West Florida Shelf (WFS) points, and (d) Chlor_a_3 with the WFS points that have been NDT-adjusted. Dashed lines are one-to-one lines and solid lines are linear regression lines in log–log coordinates.

overestimates by Chlor_a_2 at low values and underestimates at high values are comparable to additional scatter about the line associated with Chlor_a_3.

The error is reduced to 0.091 for Chlor_a_3 by removing the seven West Florida Shelf (WFS) points (Fig. 6(c)). In fact continental shelves with terrigenous runoff are not expected to exhibit typical NDT behavior. For the West Florida Shelf, upwelling of 18–20 °C water from below the Loop Current region is not unusual (Austin, 1970; Haddad and Carder, 1979), and convective overturn of surface waters in the winter is expected to refresh nutrients with water having similar thermal properties. We found that using an NDT = 19.5 °C for the seven WFS data points in the match-up dataset provided the best algorithm accuracy, lowering the error estimate when WFS points are included to RMS = 0.088 (Fig. 6(d)).

This suggests, then, that datasets rich in continental shelf data points should be scrutinized on a regional basis. If that is not possible, shelf data can be addressed using a default "global" parameter set such as given in Carder et al. (1999), that minimizes extreme excursions due to the package effect.

The RMS error values are converted to linear equivalents by

$$\mathrm{RMS}_{\mathrm{lin}} = 0.5 \cdot [(10^{\mathrm{RMS}} - 1) + (1 - 10^{-\mathrm{RMS}})] \qquad (14)$$

providing $\mathrm{RMS}_{\mathrm{lin}}$ values for data in Fig. 6 of 41%, 40%, 21%, and 20%, respectively. These results are excellent, with nearly all values reaching the 35% goal set for MODIS chlorophyll-*a* accuracies. Without stations from continental shelves, the accuracies easily surpass goal values for Chlor_a_3. With local NDT adjustments for coastal stations, sub-25% error values also appear attainable from Chlor_a_3.

5. Conclusions

MODIS Terra retrievals of chlorophyll-*a* using reprocessed Collection 4 data from SeaWiFS-like Chlor_a_2 and semi-analytical Chlor_a_3 data are accurate to better than 41%. Removing data points from continental shelves improves Chlor_a_3 accuracies to 21%, while adjusting them with more appropriate nitrate-depletion temperatures improves accuracies to about 20%. Regional inaccuracies can be higher, especially for Chlor_a_2 retrievals from upwelling and high-latitude regions, where underestimates compared to ship and Chlor_a_3 data can approach a factor of two. Chlor_a_2 retrievals in northern mid-latitude waters rich in gelbstoff may somewhat overestimate Chlor_a_3 retrievals and may be offset by underestimations due to the package effect in northern high-latitude waters.

Although validation stations encompass a wide range of environmental settings, with chlorophyll-*a* concentrations ranging from ~0.1 to 1.5 mg m^{-3}, data from many parts of the ocean and especially the central gyre regions are yet to be assessed. Initial results from January to June 2001, however, are very encouraging, especially for upwelling (California Current and equatorial Pacific) and high-latitude (Southern Ocean) locations. The data quality for normalized water-leaving radiance values from November 2000 to February 2002 are valid at Stage 1. For this reason the validity of chlorophyll-*a* retrievals presented here is likely to

also extend to the period November 2000 to February 2002.

Acknowledgements

K.L.C. gratefully acknowledges MODIS match-up data provided by F. Chavez and D. Siegel. Funding for this work was provided by the National Aeronautics and Space Administration (NAS5-31716).

References

Austin, H.M. The Florida Middle Ground. Mar. Pollution Bull. 2, 171–172, 1970.

Behrenfeld, M.J., Falkowski, P.G. Photosynthetic rates derived from satellite-based chlorophyll-*a* concentration. Limnol. Oceanogr. 42, 1–20, 1997.

Bricaud, A., Babin, M., Morel, A., Claustre, H. Variability in the chlorophyll-specific absorption coefficients of natural phytoplankton: analysis and parameterization. J. Geophys. Res. 100, 13,321–13,332, 1995.

Carder, K.L., Chen, F.R., Lee, Z.P., Hawes, S.K., Kamykowski, D. Semianalytic Moderate-Resolution Imaging Spectrometer algorithms for chlorophyll-*a* and absorption with bio-optical domains based on nitrate-depletion temperatures. J. Geophys. Res. 104, 5403–5421, 1999.

Esaias, W.E., Abbott, M.R., Barton, I., Brown, O.B., Campbell, J.W., Carder, K.L., Clark, D.K., Evans, R.H., Hoge, F.E., Gordon, H.R., Balch, W.M., Letelier, R., Minnett, P.J. An overview of MODIS capabilities for ocean science observations. IEEE Trans. Geosci. Remote Sens. 36, 1250–1265, 1998.

Esaias, W., Abbott, M., Carder, K., Campbell, J., Clark, D., Evans, R., Gordon, H., Brown, O., Minnett, P., Kearns, E., Kiipatrick, K., Mitchell, B.G., Turpie, K.R., Woodward, R., Vogel, R., Thomas, D. Ocean primary production estimates from Terra MODIS and their dependency on satellite chlorophyll-*a* algorithms. Remote Sensing Environ. (submitted).

Gordon, H.R., Morel, A. Remote Assessment of Ocean Color for Interpretation of Satellite Visible Imagery: A Review. Springer, New York, 1983.

Haddad, K.D., Carder, K.L. Oceanic intrusions: one possible initiation mechanism of red tide blooms on the west coast of Florida, in: Taylor, D.L., Seliger, H.H. (Eds.), Toxic Dinoflagellate Blooms. Elsevier, New York, pp. 269–274, 1979.

Howard, K.L., Yoder, J.A. Contribution of the subtropical ocean to global primary production, in: Liu, C.-T. (Ed.), Space Remote Sensing of the Sub-tropical Oceans. Pergamon, New York, pp. 157–168, 1997.

Hu, C., Carder, K.L., Müller-Karger, F. Atmospheric correction of SeaWiFS imagery over turbid coastal waters: a practical method. Remote Sensing Environ. 74, 195–206, 2000.

Kahru, M., Mitchell, E.G. Empirical chlorophyll algorithm and preliminary SeaWiFS validation for the California Current. Int. J. Remote Sensing 20, 3423–3429, 1999.

Kamykowski, D. A preliminary biophysical model of the relationship between temperature and plant nutrients in the upper ocean. Deep Sea Res. A 34, 1067–1079, 1987.

McClain, C.R., Barnes, R.A., Eplee Jr., R.E., Franz, B.A., Hsu, N.C., Patt, F.S., Pietras, C.M., Robinson, W.D., Schieber, B.D., Schmidt, G.M., Wang, M., Bailey, S.W., Werdell, P.J. In: Hooker, S.B., Firestone, E.R. (Eds.), SeaWiFS Postlaunch Calibration and Validation Analyses, Part 2. NASA Tech. Memo. 2000-206892, vol. 10. NASA Goddard Space Flight Center, Greenbelt, MD, 57pp, 2000.

Maynard, N.G., Clark, D.K. Satellite color observations of Spring blooming in Bering Sea shelf waters during the ice edge retreat in 1980. J. Geophys. Res. 92, 7127–7139, 1987.

Mitchell, B.G., Holm-Hansen, O. Bio-optical properties of Antarctic waters: differentiation from temperate ocean models. Deep Sea Res. A 38, 1009–1028, 1991.

Mitchell, B.G., Brody, E.A., Holm-Hansen, O., McClain, C., Bishop, J. Light limitation of phytoplankton biomass and macronutrient utilization in the Southern Ocean. Limnol. Oceanogr. 36, 1662–1677, 1991.

Moisan, T.A., Mitchell, B.G. Photophysiological acclimation of Phaeocystis antarctic Karsten under light limitation. Limnol. Oceanogr. 44, 247–258, 1999.

Moore, J.K., Abbott, M.R, Richman, J.G., Smith, W.O., Cowles, T.J., Coale, K.H., Gardner, W.D., Barber, R.T. SeaWiFS satellite ocean color data from the Southern Ocean. Geophys. Res. Lett 26, 1465–1468, 1999.

Morel, A. Optical properties of pure water and pure sea water, in: Jerlov, N.G., Nielsen, E.S. (Eds.), Optical Aspects of Oceanography. Academic Press, London, pp. 1–24, 1974.

Morel, A., Bricaud, A. Theoretical results concerning light absorption in a discrete medium, and application to specific absorption of phytoplankton. Deep-Sea Res. 28, 1375–1393, 1981.

Morel, A., Gentili, B. Diffuse reflectance of oceanic waters, II, Bidirectional aspects. Appl. Opt. 32, 6864–6879, 1993.

Morel, A., Prieur, L. Analysis of variations in ocean color. Limnol. Oceanogr. 22, 709–722, 1977.

Murphy, L.S., Haugen, E.M. The distribution and abundance of phototrophic ultraplankton in the North Atlantic. Limnol. Oceanogr. 30, 47–58, 1985.

Odate, T., Maita, Y. Regional variation in the size composition of phytoplankton communities in the Western North Pacific Ocean. Biol. Oceanogr. 6, 65–77, 1988.

O'Reilly, J.E., Maritorena, S., Siegel, D.A., et al. Ocean color chlorophyll-*a* algorithms for SeaWiFS, OC2 and OC4: Version 4, in: Hooker, S.B., Firestone, E.R. (Eds.), SeaWiFS Postlaunch Calibration and Validation Analyses, Part 3. NASA Tech. Memo. 206892, vol. 11. NASA Goddard Space Flight Center, Greenbelt, MD, pp. 9–23, 2000.

Pope, R.M., Fry, E.S. Absorption spectrum (380–700 nm) of pure water, II. Integrating cavity measurements. Appl. Opt. 36, 8710–8723, 1997.

Roesler, C.S., Perry, M.J., Carder, K.L. Modeling in situ phytoplankton absorption from total absorption spectra in productive inland marine waters. Limnol. Oceanogr. 34, 1510–1523, 1989.

Sathyendranath, S., Cota, G., Stuart, V., Maass, H., Platt, T. Remote sensing of phytoplankton pigments: a comparison of empirical and theoretical approaches. Int. J. Remote Sensing 22, 249–273, 2001.

Sedwick, P.N., Blain, S., Queguiner, B., Griffiths, F.B., Fiala, M., Bucciarelli, E., Denis, M. Resource limitation of phytoplankton growth in the Crozet Basin, Subantarctic Southern Ocean. Deep-Sea Res. II 49, 3327–3349, 2002.

Smyth, T.J., Groom, S.B., Cummings, D.G., Llewellyn, C.A. Comparison of SeaWiFS bio-optical chlorophyll-*a* algorithms within the OMEXII programme. Int. J. Remote Sensing 23, 2321–2326, 2002.

Werdell, P.J., Bailey, S.W. The SeaWiFS Bio-Optical Archive and Storage System (SeaBASS): current architecture and implementation, in: Fargion, G.S., McClain, C.R. (Eds.), NASA/TM-2002-211617. Goddard Space Flight Center, Greenbelt, MD, 45 pp, 2002.